International Journal of Modern Manufacturing Technologies
ISSN 2067–3604, Vol. XIV, No. 3 / 2022
https://doi.org/ 10.54684/ijmmt.2022.14.3.76

SOLAR RADIATION SIMULATION DEVICE FOR INVESTIGATION OF THERMAL AND PHOTOVOLTAIC PANELS

Sebastian Valeriu Hudisteanu, Cristian Nelu Chereches, Florin Emilian Turcanu, Nicolae Taranu, Marina Verdes, Ana Diana Ancas, Iuliana Hudisteanu, Dragos Ungureanu, Razvan Andrei Polcovnicu

"Gheorghe Asachi" Technical University of Iasi, Faculty of Civil Engineering and Building Services

Corresponding author: Sebastian Valeriu Hudisteanu, sebastian.hudisteanu@tuiasi.ro

Abstract: The paper presents the design and execution of a solar radiation simulation device, which ensures the adequate operation of thermal and photovoltaic panels by using light sources which have a spectrum close to the one produced by sun at minimum investment costs. The equipment is used for the experimental tracking of the behaviour of photovoltaic panels and solar thermal panels for both short and longer time intervals. The solar radiation simulation device has been developed to provide the radiation necessary for the evaluation of the efficiency and the heating of the solar panels exposed to sun. A system consisting of six OSRAM Ultravitalux 300W high-pressure lamps has been adopted, offering an optimized solution, both qualitatively and economically. The main steps achieved during its execution were: design, pre-dimensioning, verification, final dimensioning, execution and testing. According to the final tests, it was concluded that the proposed device can provide the quantitative and qualitative parameters required for solar radiation simulation in case of laboratory tests.
Key words: solar radiation, photovoltaic panels, simulation, thermal response.

1. INTRODUCTION

The solar energy is emitted in all directions and only $0.5 \cdot 10^{-9}$ of it reaches our planet [1]. The Sun is emitting both electromagnetic radiation and solar wind [2]. The average power received from the Sun at the surface of the Earth is called the solar constant and has a value of 1361 W/m^2, according to [3, 4], and 1367 W/m^2, according to [5]. Approximately 34% of solar energy is reflected back in space by snow and clouds [6], while the rest of the energy lead to the warming of the Earth's surface. The unit of measurement of solar radiation in the International System (SI) is [W/m^2], but other units are also used: [kWh/m$^2 \cdot$day], [kWh/m$^2 \cdot$year] or [kcal/m$^2 \cdot$h] [7].

Depending on the source, incident radiation on a sky-oriented surface may be of three types [2]:
- solar radiation - represented by the radiation emitted by the Sun;
- terrestrial radiation - the radiation emitted by Earth;
- atmospheric radiation - represented by the radiation emitted by the Earth's atmosphere.

Depending on the direction, the radiation is classified in [2]:
- descending radiation - composed of the solar and atmospheric radiation, which are directed to the Earth's surface;
- ascending radiation - the radiation emitted or reflected by the surface of the Earth, having an opposite direction to the first one.

In terms of photovoltaic or thermal conversion, the descending solar radiation has the greatest importance.

1.1. Solar coordinates

The position of the Sun in the sky determines the intensity of radiation and it is constantly changing, due to the rotation of the Earth around its own axis and around the Sun. It may be characterized at any one time by three angles (figure 1):
- elevation angle (altitude);
- azimuthal angle;
- the angle of inclination.

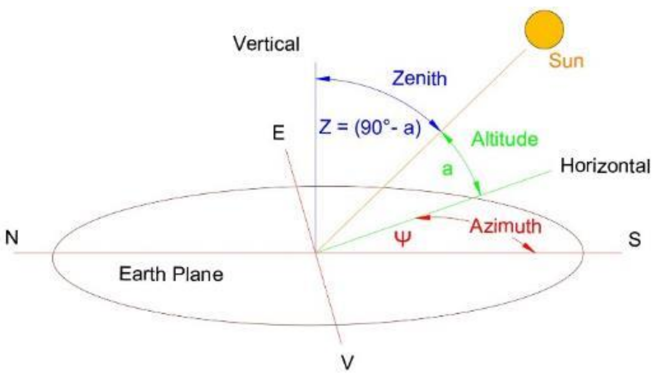

Fig. 1. Angles that characterize the position of the sun in the sky

The position of the Earth relative to the Sun is varying during the entire year according to figure 2. This path determines a variation of the Sun position and distance to Earth opposite for each hemisphere.

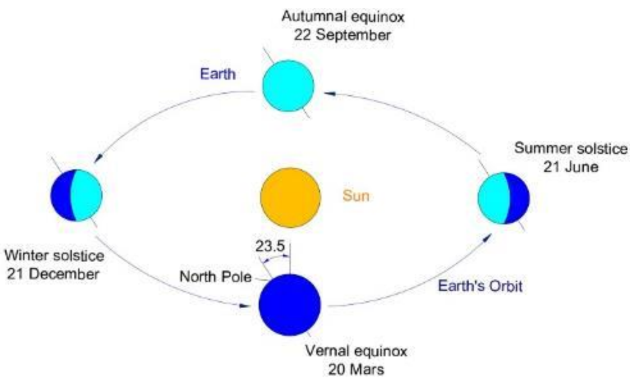

Fig, 2. Earth's position relative to the Sun over a year

1.2. Spectrum of solar radiation

The electromagnetic spectrum emitted by the Sun is 98% in the range of 0.15 ... 4.0 μm, the amount of solar energy exceeding these values being almost insignificant. Solar radiation with wavelengths greater than 3 μm is almost fully absorbed by vapor from the Earth's atmosphere. Visible radiation is a narrow range of the radiant spectrum emitted by the Sun (0.38 – 0.75 μm). Solar radiation is part of the electromagnetic radiation waves, having all their properties and characteristics. Thus, based on the photon energy formula (1) and since the frequency $f = c/\lambda$ (c is the speed of light) it can be stated the wavelength, λ, of the solar radiation is inversely proportional to the frequency and the energy, E [8].

$$E = \frac{h \cdot c}{\lambda} = hf \quad (1)$$

in which h is the Planck constant.

The spectrum of solar radiation on the Earth's surface presents some differences comparing to the solar radiation from cosmic space, due to the atmosphere interfering. The electromagnetic energy emitted by the Sun, classified by the wavelength, can be expressed as ultraviolet, visible and infrared radiation, [8, 9].

The main components of solar radiation are: direct, diffuse, global and reflected radiation. The capacity of a surface to reflect solar radiation is known as albedo.

The air mass (AM) index is a measure of the degree of absorption of radiant energy from the Earth's atmosphere as it passes through it [3], figure 3.

$$AM = \frac{1}{sin\gamma_S} = \frac{1}{cosZ} = \frac{L}{L_O} \quad (2)$$

where,

Lo - the path of solar radiation to sea level when the sun is at the zenith [m];

Z – zenith angle [°];

L - the actual path of solar radiation through the atmosphere for the zenith angle Z.

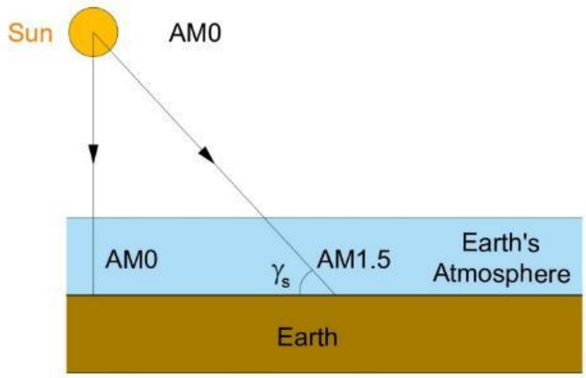

Fig. 3. Calculation of the air mass index

The reference values of the air mass index are, figure 4:

AM0 – at the upper limit of the Earth's atmosphere; G = 1353 W/m^2;

AM1 – the sun perfectly vertical, at sea level, horizontal surface, G =1000 W/m^2;

AM1.5G – surface inclined to 37°, zenith 48°, oriented S, albedo 0.3, turbidity 0.29, ambient temperature of 20 °C, G = 963.8 W/m^2;

AM2 – zenith 60°.

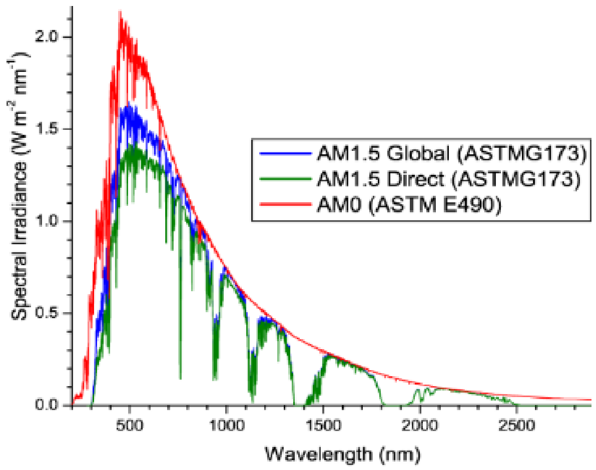

Fig. 4. The solar radiation spectrum at AM0, AM1.5D and AM1.5G [11]

2. SIMULATION OF SOLAR RADIATION

In literature there are presented two main types of solar simulators for photovoltaic cell testing: Steady State (SS) and Pulsed Simulator (PS), [11]. SS simulators are used to test photovoltaic panels in continuous operation, to test their behaviour at elevated temperatures and various cooling or aging solutions [12]. Instead, the PS type are used to determine the functionality and instantaneous efficiency of photovoltaic cells – for example in standard test conditions (STC) analysis.

Most solar simulators use Xenon or halogen filtered light sources, [13]. The light sources used are based on phenomena of incandescence and luminescence [2].

The solar radiation intensity for a solar simulator with AM1.5G filter is 1000 W/m^2 and is called "1 Sun" [11]. The radiation emitted by a solar simulator is evaluated from three perspectives: spectral match, spatial uniformity and temporal stability, [14, 15].
Spectral match is the approximation of the spectrum produced by the solar simulator compared to the AM1.5G spectrum, considered the spectrum of global solar radiation.
Space uniformity refers to the uniformity of illumination produced by the solar simulator on a given surface. This property is very important and difficult to reach, even for professional devices, taking into account the high uniformity of the solar radiation.
Temporal stability is a measure of light beam stability over a very short period of time, approximately 1 second, according to [14].
These characteristics are classified into three classes: A, B, C, according to table 1.

Table 1. Solar simulators classes [14, 15].

Class	Spectral match	Spatial non-uniformity	Temporal instability
A	0.75...1.25	2%	2%
B	0.6...1.4	5%	5%
C	0.4...2.0	10%	10%

Although the thermal effect of simulated radiation is easy to simulate, on the other hand, for testing silicon photovoltaic cells, the radiation integrals are imposed at certain emitted wavelengths. These percentages are shown in Table 2, for the AM1.5G and AM1.5D for terrestrial spectrum and AM0 for the outer space spectrum.

Table 2. The radiation integrals required for testing silicon photovoltaic cells [16]

Wavelength (nm)	AM1.5D	AM1.5G	AM0
300–400	-	-	8,0%
400–500	16.9%	18.4%	16.4%
500–600	19.7%	19.9%	16.3%
600–700	18.5%	18.4%	13.9%
700–800	15.2%	14.9%	11.2%
800–900	12.9%	12.5%	9.0%
900–1100	16.8%	15.9%	13.1%
1100–1400	-	-	12.2%

According to international standards [14, 15], a solar simulator is a device that simulates solar radiation and solar spectrum of the minimum C class.
To simulate solar radiation, in the case of simpler applications, there are solutions proposed and tested in the literature [13]. Most often, electric lamps which are emitting in a spectrum that is close to that of solar radiation are used, but with a much lower accuracy than compact solar simulators, [17].
The most common source of solar radiation simulation is the xenon arc lamp with filters installed to approximate the AM1.5G spectrum, [18]. This type of lamp provides a reasonable spectral match, even when no filters are used. Even the spectrum of xenon lamps is characterized by various bands with peak wavelengths, causing errors when used for finesse applications, it may be considered appropriate for larger scale applications regarding the solar thermal or photovoltaic panels, [19, 20]. Arc xenon lamps can be used for both high-power and low-power installations, or for variable illumination intensities, [10].
Also, for simple tests, the halogen lamp with a dichroic filter can also be used. Due to the fact that the lamp filament has a temperature of less than 6000 K, it produces a spectrum with more infrared radiation and less ultraviolet radiation. This problem can be partially solved by using a reflector that allows the passage of infrared radiation and reflects visible and ultraviolet radiation. The advantage of halogen lamps is the superior temporal stability to those with xenon [10].
The quartz tungsten halogen (QTH) lamp creates a spectrum very close to the radiation emitted by the black body, even if the colour temperature is lower than the Sun, [21].
Metal halide lamps (MHL) were originally developed for cinema applications, but they are also used to simulate solar radiation. These are used in literature papers to test photovoltaic or hybrid panels, [17].
Light emitting diode (LED) lamps have a significant development lately, with good prospects for simulating solar radiation, [13]. Thus, lighting sources can be obtained by combining LEDs of various colours to obtain a reasonable spectrum, [22].
Generally, the more a solar simulator approaches the spectrum of solar radiation, the more expensive it gets. To achieve a conventional handmade solar radiation simulation equipment, an optimal calculation between accuracy and cost must be conducted. Therefore, if no maximum spectrum tolerance is specified, a xenon lamp can be used instead of a professional solar simulator, [19]. An important aspect in simulating solar radiation is to obtain a reasonable level of illumination, as uniform as possible, on the surface of the solar thermal or photovoltaic panel.
A less expensive solution than professional solar simulators to obtain a spectrum close to that of solar radiation may be the simultaneous use of two or more light sources emitting in complementary spectra.
In this paper there are presented the steps followed in the development of a solar radiation simulation device and it is not focused on professional solar simulators, defined according to [14, 15].

3. DESIGN AND CONSTRUCTION OF THE SOLAR RADIATION SIMULATION DEVICE

For endurance tests or to assess the thermal behaviour of solar thermal and photovoltaic panels, light sources with lower spectral matching may be used and subsequent error correction calculations, [19-21]. This technique, which is common for solar simulators, is also used to build the device presented below.

The solar simulation device is designed for the experimental tracking of the behaviour of photovoltaic panels and solar thermal panels for both short and long periods. The device has been developed to provide both radiation necessary for the photovoltaic panel conversion and also thermal radiation to simulate the heating effect of the solar panels exposed to sun. Therefore, the implementation of a system consisting of six OSRAM Ultravitalux 300W high-pressure lamps has been adopted, figure 4 and table 3, offering an optimized solution, both qualitatively and economically.

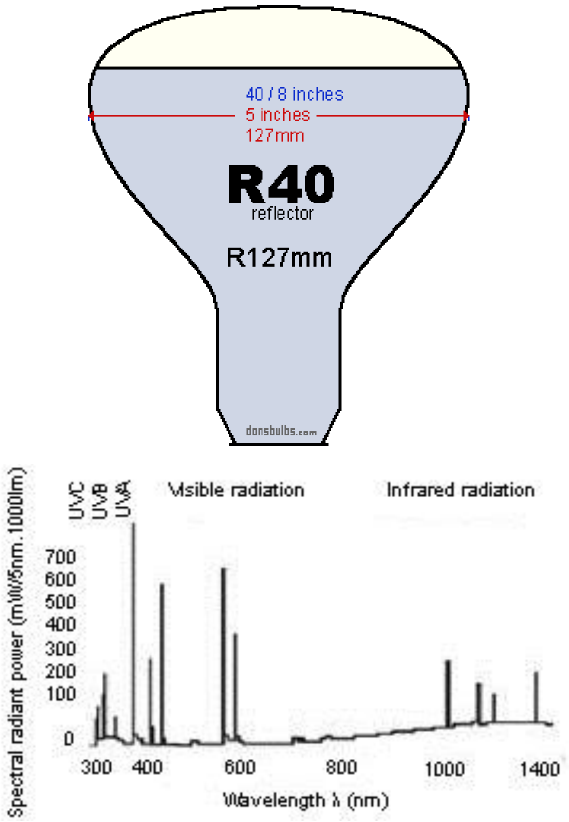

Fig. 4. OSRAM Ultra-Vitalux 300 W lamp [23] a) geometry; b) electromagnetic spectrum emitted by the lamp λ

Table 3. Datasheet information of light source [23]

	Power = 300 W; Socket = E27; Operating time = 1000 h; Emission = UVA + UVB, visible, IR; Diameter = 127 mm; Length = 185 mm.

The main requirements imposed for the solar radiation simulation device were:

- uniform intensity of radiation generated and possibility of variation the incident flux;
- obtaining a radiation spectrum convertible by photovoltaic cells;
- obtaining a distribution of radiation as uniform as possible;
- limitation of device dimensions for compatibility with future experimental set-ups (maximum height 1 m, maximum width 0.7 m) and solar thermal and photovoltaic panels (0.50 m x 0.70 m)
- ensuring electrical safety and the possibility of command;
- ensuring adequate rigidity and handling.

In the first phase, the intensity of incident radiation from a single lamp was tested, the measurements being made on a circular incidence contour, figure 5.

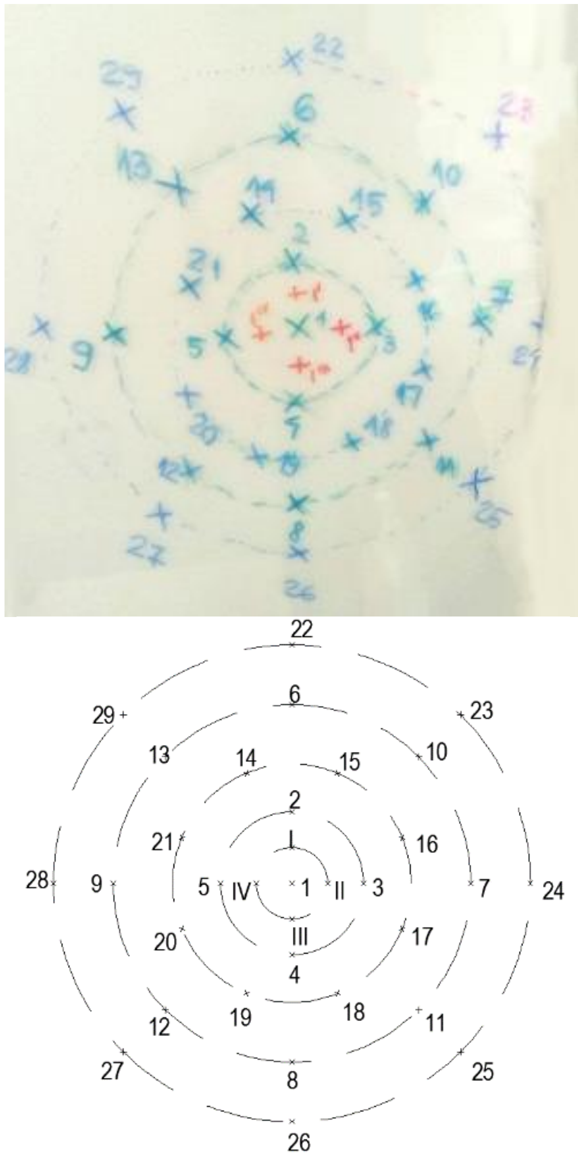

Fig. 5. Set-up of radiation measurement points for 1 light source a) experimental measurements; b) graphical representation

The radiation produced by the light sources was determined using the following devices specific for measuring the intensity of solar radiation: - Pyranometer Voltcraft PL-110SM [24], Solarimeter - P.A. Hilton LTD RE550 [25].

The results of the radiation measurements are shown in figure 6. Taking into account these values and the limitations presented above, the adequate number and position of the lamps was determined.

Figure 7 shows the radiative flux emitted by a single light source depending on the distance, on the horizontal axis - figure 7a and on the vertical axis - figure 7b.

By combining the above results, figure 6 and figure 7, the optimal solution for the simulation device was determined. It is composed of six light sources, symmetrically arranged, on two vertical and three horizontal lines. The sketch of the proposed device is shown in figure 8.

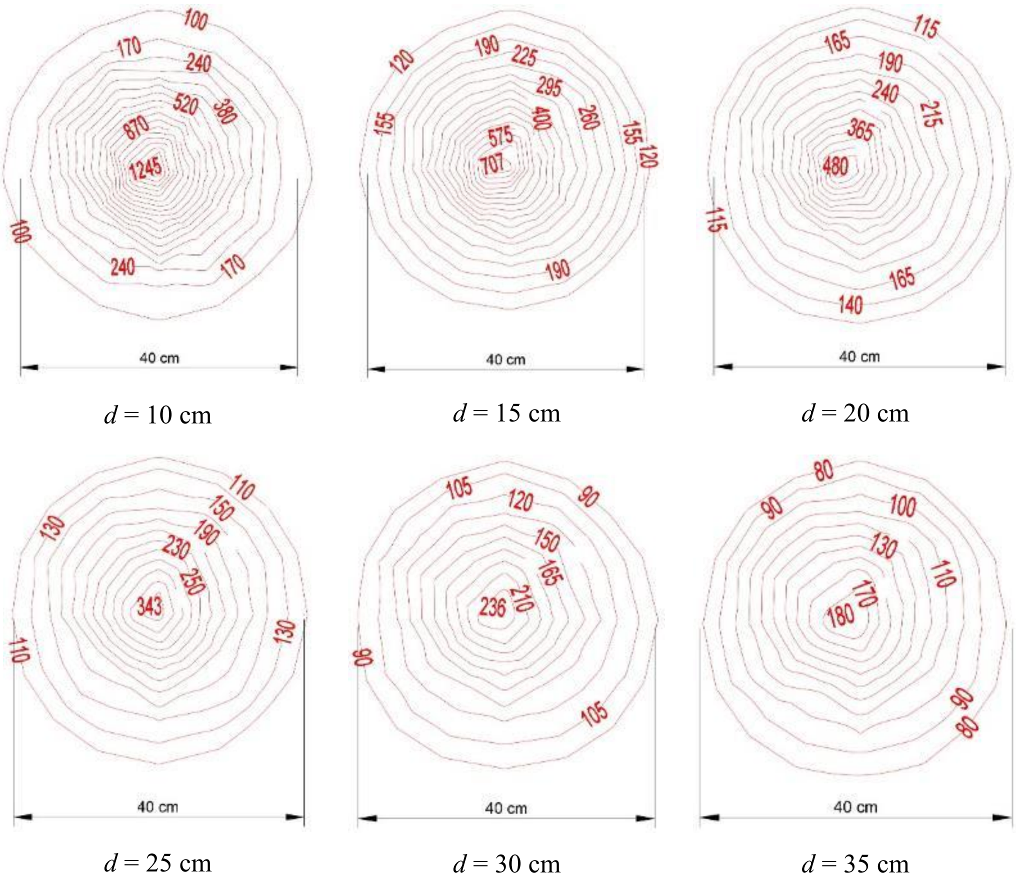

Fig. 6. Results of radiation measurement [W/m^2] depending on distance (d) for 1 light source

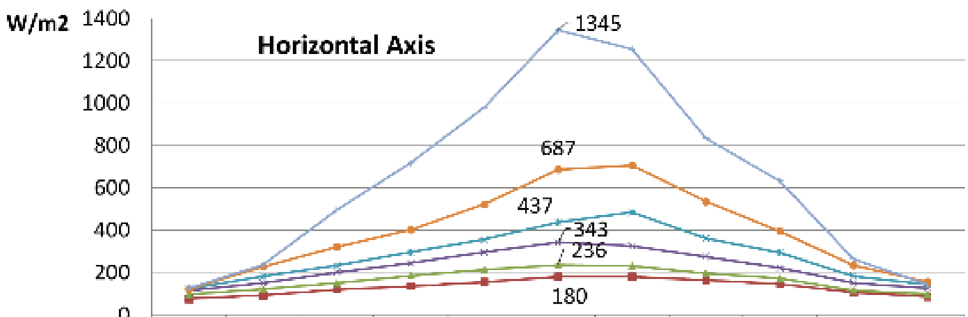

	1	2	3	4	5	6	7	8	9	10	11
Distance to center [cm]	20	15	10	6	3	0	3	6	10	15	20
d = 35 cm	76	92	120	135	156	180	180	164	145	105	85
d = 30 cm	96	121	150	185	213	236	232	196	172	115	99
d = 25 cm	115	150	200	244	296	343	326	275	222	150	125
d = 20 cm	124	181	233	296	356	437	484	362	295	183	144
d = 15 cm	122	227	322	402	522	687	707	536	396	234	156
d = 10 cm	126	236	496	717	980	1345	1255	835	633	263	144

a)

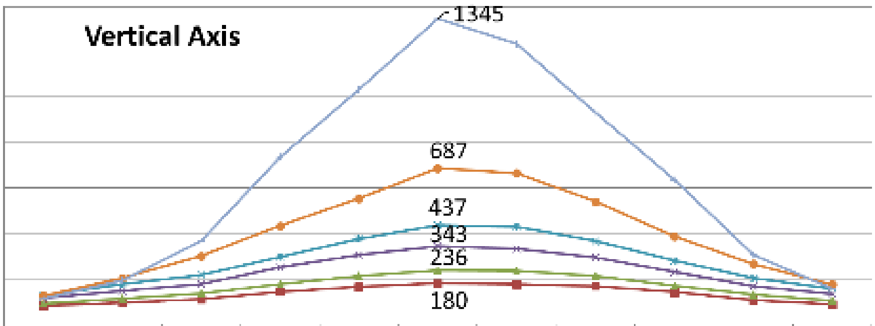

1	2	3	4	5	6	7	8	9	10	11
20	15	10	6	3	0	3	6	10	15	20
80	95	110	143	164	180	176	167	142	106	87
91	113	136	176	213	236	234	213	169	130	104
116	146	176	250	304	343	332	294	230	166	132
123	176	216	296	376	437	430	365	279	203	156
124	203	300	433	553	687	665	540	386	265	174
112	192	366	735	1033	1345	1234	932	635	305	156

b)

Fig. 7. The radiative flux emitted by 1 light source a) on the horizontal axis; b) on the vertical axis

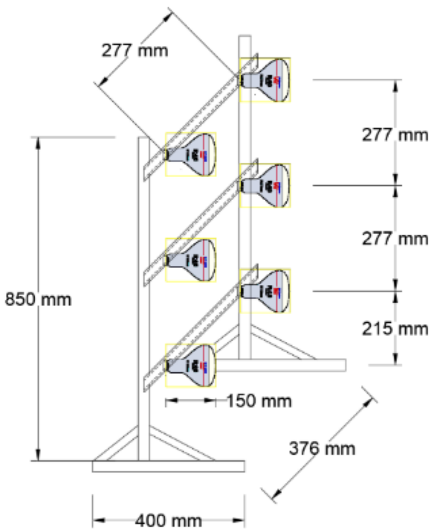

Fig. 8. Sketch of the solar radiation simulation device

Based on the proposed device, a predictive analysis was performed and the radiative flux to be produced by the solar radiation simulation device was determined. The results of predictive analysis of the radiative flux are shown in figure 9.

It is noted that the presumed radiative flux generated for the proposed configuration ensures a reasonable uniformity of the incident radiation and the dependence of the values on the distance from the working plane. Also, the minimum use distance of the device will be 15 cm, because for smaller distances radiation values above 1000 W/m^2 are reached and the incident radiative flux is very irregular.

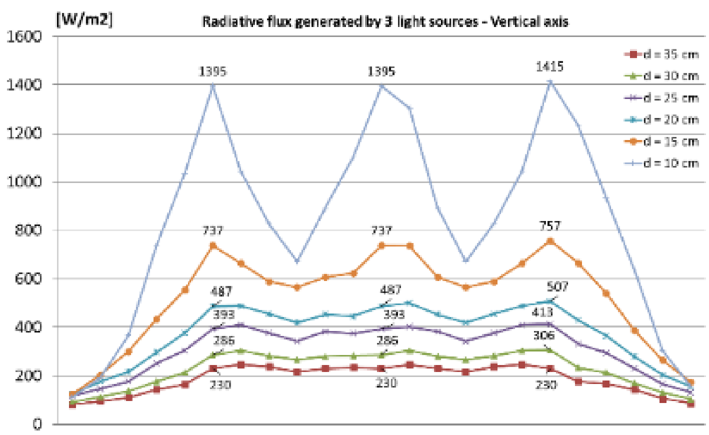

a)

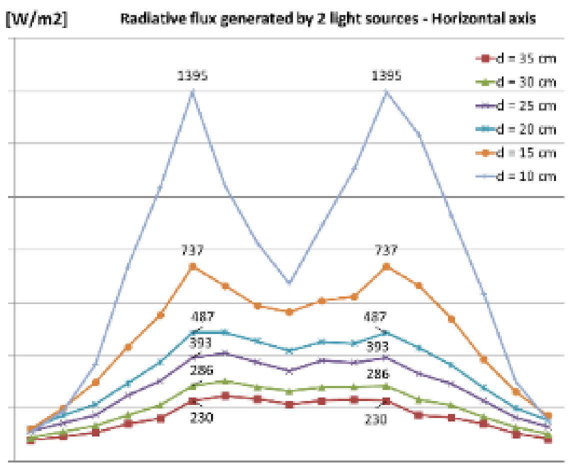

b)

Fig. 9. Predicting the radiative flux distribution for the proposed device: a) on the vertical axis; b) on the horizontal axis

4. CONSTRUCTION AND TESTING OF THE SOLAR RADIATION SIMULATION DEVICE

Figure 10 shows some representative images of the components during the execution of the solar simulation device. The main execution steps were to realize the support frame, connect the E27 sockets, mount the reflective plate, light source mounting, electrical connections and functional testing.

Fig. 10. Execution steps (a - support frame, b - E27 socket; c - reflective plate positioning, d - light source mounting, e - electrical connections, f - functional testing)

Given that the chosen light sources are not dimmable [23], the variation of the radiative flux of the simulation device is achieved by variation the distance between the lamps and the incidence plan. Examination of the radiative flux from the proposed simulator confirmed the data from the pre-dimensioning stage, the average values being in the range of 260 and 545 W/m^2 - figure 11.

The surface of PV panel was provided with 23 measuring points (numbered from 21 to 43) for different distances between the solar simulating device and incident surface. The results are presented in figure 12.

The spectral match has been evaluated by comparing the entire spectrum of radiation of the simulator with the reference solar radiation.

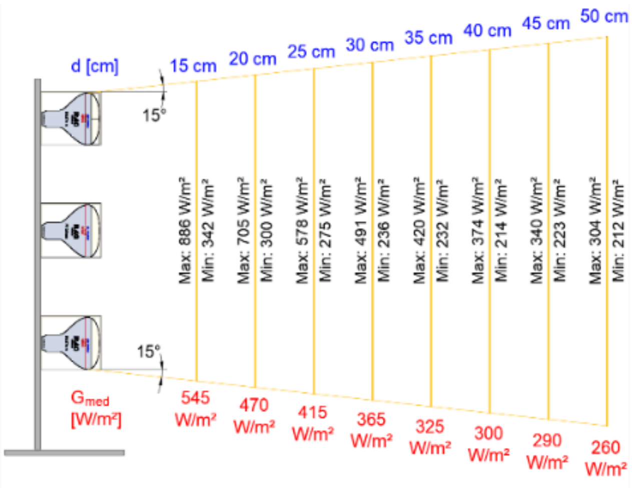

Fig. 11. Measurement of the radiation produced by the solar radiation simulation device depending on distance – minimum, maximum and average values

Taking into account the data presented in table 4, the present solar simulation device could be assimilated as being close to class C solar simulator, which is satisfactory for experimental testing the PV or PV/T panels [26-30].

In this regard, the productivity of a reference PV panel was evaluated for the same levels of outdoor solar radiation and that produced by using the present device – table 4.

The evaluation of the solar radiation simulation device was realized both for solar thermal panels and monocrystalline and polycrystalline photovoltaic panels. In table 4 it can be analysed the average response of these panels to radiation produced by simulation device compared to natural solar radiation.

As expected, the main characteristics of the simulation device (intensity and uniformity of the radiation) are varying inversely proportionally – Table 4.

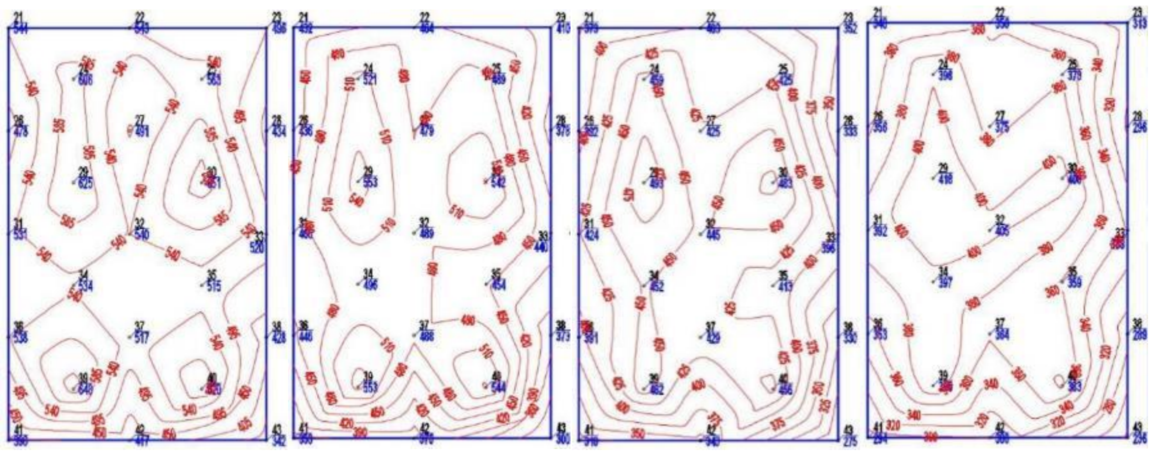

a) 15 cm b) 20 cm c) 25 cm d) 30 cm

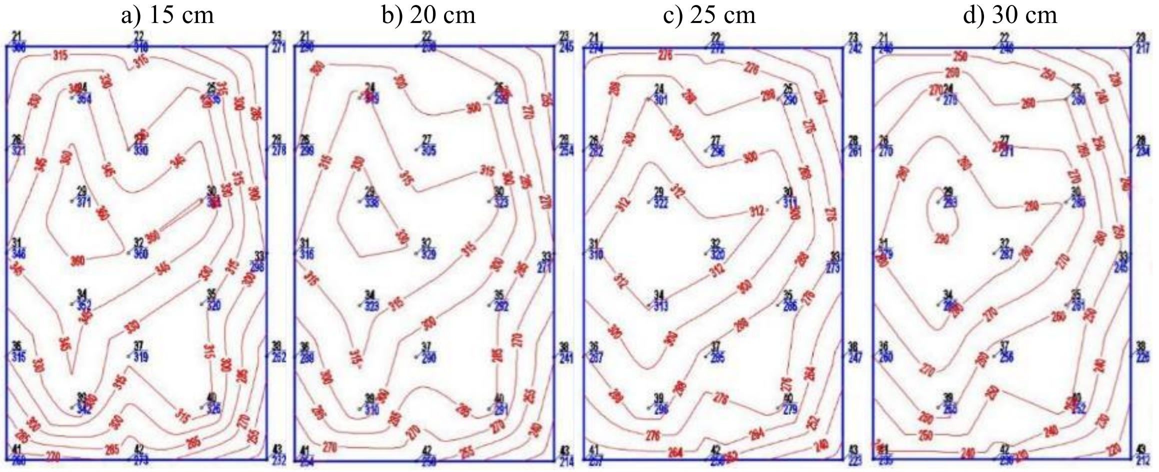

a) 35 cm b) 40 cm c) 45 cm d) 50 cm

Fig. 12. Distribution of the radiation levels on the surface of PV panel for various distances between the solar simulation device and incident plane

Table 4. Evaluation of the quality of the radiation produced by the solar simulation device

Distance	Spectral match	Thermal response	Spatial non-uniformity
15 cm	81.88 %	96.63%	19.45%
20 cm	84.77 %	95.67%	18.80%
25 cm	86.23 %	95.10%	17.66%
30 cm	88.45 %	94.25%	14.52%
35 cm	89.64 %	93.32%	14.15%
40 cm	90.88 %	91.49%	12.69%
45 cm	93.54 %	90.59%	12.67%
50 cm	95.12 %	90.13%	11.03%

5. CONCLUSIONS

The obtained experimental results confirm that the proposed device can provide appropriate quantitative and qualitative parameters required for simulation of solar radiation for laboratory testing of the photovoltaic and solar thermal panels.

The maximum average radiative flux produced by device, 545 W/m^2, is adequate for the experimental set-ups regarding the integration of PV panels on the building's facades or roofs.

The present device has been used successfully for long term simulation of solar radiation effect over photovoltaic (in order to test cooling techniques) and also for solar thermal panels.

6. ACKNOWLEDGEMENT

This work was supported by a grant of the Romanian Ministry of Education and Research, CCCDI-UEFISCDI, project number PN-III-P2-2.1-PED-2019-1294, within PNCDI III.

7. REFERENCES

1. Richter, C., Lincot, D., Gueymard, C., (2012). *Solar Energy*, Springer, New York.
2. Oprea, C., (2005). *Radiația solară, aspecte teoretice și practice* ISBN 973–03915-1, Bucharest.
3. ASTM E-490-00a (2014). *Standard Solar Constant and Zero Air Mass Solar Spectral Irradiance Tables*.
4. https://sunclimate.gsfc.nasa.gov/article/solar-irradiance#:~:text=Satellite%20TSI%20measurements%20have%20enabled,meter%20(W%2Fm2) last accessed on: 01.02.2022.
5. library.wmo.int/doc_num.php?explnum_id=9416 last accessed on: 01.02.2022.
6. Spellman, F.R., Stoudt, M.L., (2013). *Environmental Science: Principles and Practices*, Lanham, MD: Government Institutes Press.
7. http://www.eere.energy.gov, last accessed on: 01.02.2022.
8. IEC 904-7 *Computation of Spectral Measurement of a PV Device*.
9. IEC 904-8 *Guidance for Spectral Measurement of a PV Device*.
10. https://www.pveducation.org, last accessed on: 01.02.2022.
11. Mantosh, K.C., (2014). *A step by step guide to selecting the "right" Solar Simulator for your solar cell testing application*, Photo Emission Tech. Inc.
12. Tolvanen, A., Oy, E., (2011). *Solar Simulation Standards and QuickSun Measurement System*. https://wonwoosystem.co.kr/pic/catalog/Solar%20Simulation%20Standards%20and%20QuickSun%20Measurement%20System.pdf, last accessed on: 01.02.2022.
13. Kohraku, S., Kurokawa, K., (2003). *New methods for solar cells measurement by led solar simulator*, 3rd World Conference on Photovoltaic Energy Conversio, Osaka, Japan, 1977-1980, https://ieeexplore.ieee.org/stamp/stamp.jsp?tp=&arnumber=1306332, last accessed on: 01.02.2022.
14. ASTM E927-10 (2015). *Standard Specification for Solar Simulation for Terrestrial Photovoltaic Testing*.
15. IEC 60904-9 (2007). *Photovoltaic devices - Part 9: Solar simulator performance requirement*.
16. https://www.newport.com/n/solar-simulator-sample-calculations, last accessed on: 01.02.2022.
17. Yang, D.J., Yuan, Z.F., Lee, P.H., Yin, H. M., (2012). *Simulation and experimental validation of heat transfer in a novel hybrid solar panel*, I J of H and M Transfer, 55, 1076–1082.
18. Donga, X., Sun, Z., Nathan, G.J., Ashman, P.J., Gu D., (2015). *Time-resolved spectra of solar simulators employing metal halide and xenon arc lamps*, Solar Energy, 115, 613-620.
19. Tawfik, M., Tonnellier, X., Sansom, C., (2018). *Light source selection for a solar simulator for thermal applications: A review*, Renewable and Sustainable Energy Reviews, 90, 802-813.
20. Parupudi, R.V., Singh, H., Kolokotroni, M., (2019). *Sun Simulator for Indoor Performance assessment of Solar Photovoltaic Cells*, Energy Procedia, 161, 376-384.
21. Jenkins, R., Aldwell, B., Yin, S., Meyer, M., Robinson, A.J., Lupoi, R., (2019). *Energy efficiency of a quartz tungsten halogen lamp: Experimental and numerical approach*, Thermal Science and Engineering Progress, 13, 100385.
22. http://www.newport.com, last accessed on: 01.02.2022.
23. https://www.osram.com/ecat/ULTRA-VITALUX%20UV-A-UV-A-Ultraviolet%20lamps-Industry-Specialty%20Lighting/com/en/GPS01_1028569/ZMP_60829/, last accessed on: 01.02.2022.

24. https://www.conrad.com/p/voltcraft-pl-110sm-lux-meter-0-1999-wm-101038, last accessed on: 01.02.2022.
25. https://www.p-a-hilton.co.uk/, last accessed on: 01.02.2022.
26. Shatat, M., Riffat, S., Agyenim, F., (2013). *Experimental testing method for solar light simulator with an attached evacuated solar collector,* International Journal of Energy and Environment, 4, 219-230.
27. Jin, J., Hao, Y., Jin, H., (2019). *A universal solar simulator for focused and quasi-collimated beams,* Applied Energy, 235, 1266-1276.
28. Sabahi, H., Tofigh, A.A., Kakhki, I.M., Bungypoor-Fard, H., (2016). *Design, construction and performance test of an efficient large-scale solar simulator for investigation of solar thermal collectors*, Sustainable Energy Technologies and Assessments, 15, 35–41.
29. Hudisteanu, S.V., *Pruteanu, M., Mateescu, T.D., Vasilache, M., (2017). Experimental investigation of temperature effects on the parameters of photovoltaic panels,* Environmental Engineering & Management Journal, 16(7), 1643-1648.
30. Hudișteanu, S.V., Țurcanu, F.E., Cherecheș, N.C., Popovici, C.G., Verdeș, M., Hudisteanu, I., (2021). *Enhancement of PV Panel Power Production by Passive Cooling Using Heat Sinks with Perforated Fins,* Appl. Sci., 11, 11323.

Received: June 17, 2022 / Accepted: December 15, 2022 / Paper available online: December 20, 2022